

# Delayed Rectifier $K^+$ Currents, $I_K$ , Are Encoded by Kv2 $\alpha$ -Subunits and Regulate Tonic Firing in Mammalian Sympathetic Neurons

Sacha A. Malin and Jeanne M. Nerbonne

Department of Molecular Biology and Pharmacology, Washington University School of Medicine, St. Louis, Missouri 63110

Previous studies have revealed the presence of four kinetically distinct voltage-gated  $K^+$  currents,  $I_{Af}$ ,  $I_{As}$ ,  $I_K$ , and  $I_{SS}$ , in rat superior cervical ganglion (SCG) neurons and demonstrated that  $I_K$  and  $I_{SS}$  are expressed in all cells, whereas  $I_{Af}$  and  $I_{As}$  are differentially distributed. Previous studies have also revealed the presence of distinct components of  $I_{Af}$  encoded by  $\alpha$ -subunits of the Kv1 and Kv4 subfamilies. In the experiments described here, pore mutants of Kv2.1 (Kv2.1W365C/Y380T) and Kv2.2 (Kv2.2W373C/Y388T) that function as Kv2 subfamily-specific dominant negatives (Kv2.1DN and Kv2.2DN) were generated to probe the functional role(s) of Kv2  $\alpha$ -subunits. Expression of Kv2.1DN or Kv2.2DN in human embryonic kidney-293 cells selectively attenuates Kv2.1- or Kv2.2-encoded  $K^+$  currents, respectively. Using the Biolistics Gene Gun, cDNA constructs encoding either Kv2.1DN or Kv2.2DN [and enhanced green fluorescent protein (EGFP)] were introduced into SCG neurons. Whole-cell recordings from EGFP-

positive Kv2.1DN or Kv2.2DN-expressing cells revealed selective decreases in  $I_K$ . Coexpression of Kv2.1DN and Kv2.2DN eliminates  $I_K$  in most (75%) SCG cells and, in the remaining (25%) cells,  $I_K$  density is reduced. Together with biochemical data revealing that Kv2.1 and Kv2.2  $\alpha$ -subunits do not associate in rat SCGs, these results suggest that Kv2.1 and Kv2.2 form distinct populations of  $I_K$  channels, and that Kv2  $\alpha$ -subunits underlie (most of)  $I_K$  in SCG neurons. Similar to wild-type cells, phasic, adapting, and tonic firing patterns are evident in SCG cells expressing Kv2.1DN or Kv2.2DN, although action potential durations in tonic cells are prolonged. Expression of Kv2.2DN also results in membrane depolarization, suggesting that Kv2.1- and Kv2.2-encoded  $I_K$  channels play distinct roles in regulating the excitability of SCG neurons.

**Key words:**  $K^+$  channels;  $I_K$ ; Kv2.1; Kv2.2; Kv2.1W365C/Y380T; Kv2.2W373C/Y388T; transgenics; Gene Gun; neuronal excitability; repetitive firing patterns

Voltage-gated  $K^+$  channels are important determinants of neuronal membrane excitability, and differences in  $K^+$  channel expression patterns and densities contribute to the variations in action potential waveforms and repetitive firing patterns evident in different neuronal cell types (Pongs, 1999). Electrophysiological studies have revealed that most mammalian neurons express multiple types of voltage-gated  $K^+$  currents with distinct time- and voltage-dependent properties (Rudy, 1988; Storm, 1990). A large number of voltage-gated  $K^+$  (Kv) channel pore-forming ( $\alpha$ ) and a variety of Kv accessory subunits, thought to underlie these channels have now been identified (Coetzee et al., 1999; Pongs, 1999; An et al., 2000; Kuryshv et al., 2000), and there is presently considerable interest in defining the relationships between these subunits and neuronal voltage-gated  $K^+$  currents.

We have shown previously that sympathetic neurons isolated from the rat superior cervical ganglion (SCG) express four kinetically distinct voltage-gated  $K^+$  currents: two transient A-type currents,  $I_{Af}$  and  $I_{As}$ , a delayed rectifier current,  $I_K$ , and a steady-state current,  $I_{SS}$  (Malin and Nerbonne, 2000). Although  $I_K$  and  $I_{SS}$  are expressed in all SCG cells, the transient currents,  $I_{Af}$  and  $I_{As}$ , are differentially distributed, and SCG neurons were classified as type I ( $I_{Af}$ ,  $I_K$ ,  $I_{SS}$ ), type II ( $I_{As}$ ,  $I_K$ ,  $I_{SS}$ ) or type III ( $I_K$ ,

$I_{SS}$ ) based on the differential expression of these voltage-gated  $K^+$  currents (Malin and Nerbonne, 2000). In previous studies, we exploited molecular genetic strategies to assess the roles of  $\alpha$ -subunits of the Kv1 and Kv4 subfamilies in the generation of voltage-gated  $K^+$  currents in rat SCG cells. Recordings obtained from SCG neurons expressing the Kv4 subfamily-specific dominant negative Kv4.2W362F (Barry et al., 1998) revealed that  $I_{Af}$  is eliminated in most type I and all type II SCG cells (Malin and Nerbonne, 2000). Subsequent experiments revealed that expression of a Kv1 subfamily-specific dominant negative Kv1.5W461F (Li et al., 1999) eliminates  $I_{Af}$  in a subset of type I cells (Malin and Nerbonne, 2001), demonstrating that there are two molecularly distinct components of  $I_{Af}$ . However, the molecular correlates of  $I_K$ ,  $I_{As}$ , and  $I_{SS}$  in SCG cells have not been identified.

Previous studies suggest that  $\alpha$ -subunits of the Kv2 subfamily encode neuronal delayed rectifier currents,  $I_K$  (Baranauskas et al., 1999; Murakoshi and Trimmer, 1999; Du et al., 2000; Blaine and Ribera, 2001). In addition, both Kv2.1 and Kv2.2 are readily detected in mammalian hippocampal neurons, although these subunits are differentially targeted (Hwang et al., 1992, 1993; Maletic-Savatic et al., 1995; Du et al., 1998; Lim et al., 2000). In rat SCG neurons, Kv2.1 and Kv2.2 are expressed at the mRNA level (Dixon and McKinnon, 1996; Pankevych et al., 1999). In the experiments described here, Kv2 subfamily-specific dominant negative constructs, Kv2.1W365C/Y380T (Kv2.1DN) and Kv2.2W373C/Y388T (Kv2.2DN), were generated, characterized, and introduced into SCG neurons to test directly the hypothesis that Kv2  $\alpha$ -subunits underlie  $I_K$  and to probe the functional roles of Kv2-encoded  $K^+$  channels in shaping the waveforms of indi-

Received July 24, 2002; revised Sept. 10, 2002; accepted Sept. 10, 2002.

Financial support was provided by the National Science Foundation (predoctoral fellowship to S.A.M.) and the National Institutes of Health (NS-30676).

Correspondence should be addressed to Jeanne M. Nerbonne, Washington University Medical School, 660 South Euclid, Box 8103, St. Louis, MO 63110. E-mail: jnerbonn@peg.wustl.edu.

Copyright © 2002 Society for Neuroscience 0270-6474/02/2210094-12\$15.00/0

vidual action potentials and in regulating repetitive firing in these cells.

## MATERIALS AND METHODS

**Construction of Kv2.1W365C/Y380T and Kv2.2W373C/Y388T.** Rat Kv2.1 (obtained from R. Joho, University of Texas Southwestern, Dallas, TX) was subcloned into the pAlter vector (Promega, Madison, WI), and two pore mutations (W365C/Y380T) were introduced using the Altered Sites Mutagenesis II (pAlter) system (Promega). Codons TGG (W365) and TAC (Y380) were mutagenized to TGC (C) and ACC (T). To aid in the detection of the mutant construct, the FLAG epitope was added to the C terminus of Kv2.1W365C/Y380T by PCR. The corresponding mutations (W373C/Y388T) were also introduced into rat Kv2.2 (obtained from S. Trimmer, State University of New York, Stony Brook, NY) in pAlter using PCR. Codons TGG (W373) and TAC (Y388) were mutagenized to TGC (C373) and ACC (T388). The *myc* epitope tag was added on the C terminus of Kv2.2W373C/Y388T by PCR, and Kv2.2W373C/Y388T-*myc* was cloned into the pEF6/v5His vector (Promega). Both the Kv2.1W365C/Y380T and the Kv2.2W373C/Y388T constructs were sequenced in their entirety to ensure that no additional mutations were introduced.

**Expression studies in human embryonic kidney-293 cells.** The functional properties of Kv2.1W365C/Y380T and Kv2.2W373C/Y388T were examined in heterologous expression studies in human embryonic kidney (HEK)-293 cells. HEK-293 cells were maintained in growth medium [Eagle's Minimal Essential Medium (EMEM) (Invitrogen, San Diego, CA), containing 10% heat-inactivated fetal calf serum (FCS) and 100 U/ml penicillin–streptomycin], split, plated in 35 mm tissue culture dishes, and transfected with wild-type and mutant  $K^+$  channel  $\alpha$ -subunits [and enhanced green fluorescent protein (EGFP)] using the calcium phosphate method. For this purpose, cells were preincubated for 1 hr in transfection media (EMEM with 5% serum). In most experiments, 2–3  $\mu$ g of test DNA (1:2 ratio of EGFP to test constructs) and 7–8  $\mu$ g of carrier DNA (pSK; total of 10  $\mu$ g of DNA) were combined in 100  $\mu$ l of 0.25 M  $CaCl_2$  and 100  $\mu$ l of *N,N*-bis[2-hydroxyethyl]2-aminoethanesulfonic acid (BES)-buffered saline [containing in mM: 280 NaCl, 1.5  $Na_2HPO_4 \cdot 7H_2O$ , 50 BES (Sigma, St. Louis, MO) at pH 6.95] was then added. The resulting solution was mixed and incubated at room temperature for 15 min before being added (drop-wise) to the cells in each 35 mm culture dish. After 15 hr of incubation at 37°C, cells were washed in growth medium. Electrophysiological recordings were obtained from EGFP-positive cells 12–36 hr later. In these experiments, cells were transfected with EGFP and the following: Kv2.1, Kv2.2, Kv2.1W365C/Y380T, Kv2.2W373C/Y388T, Kv2.1 plus Kv2.1W365C/Y380T, Kv2.1 plus Kv2.2W373C/Y388T, Kv2.2 plus Kv2.2W373C/Y388T, Kv2.2 plus Kv2.1W365C/Y380T, Kv1.4, or Kv1.4 plus Kv2.1W365C/Y380T. To evaluate the functional efficacy of the mutant constructs, current densities obtained from cells transfected with the wild-type  $Kv\alpha$ -subunit (and EGFP) constructs were compared with those from cells transfected with wild-type and mutant  $Kv\alpha$ -subunit (and EGFP) constructs. These experiments were performed in parallel. In most experiments, the wild-type and mutant  $Kv\alpha$ -subunits were used at a 1:1 ratio, and the same absolute amount of wild-type cDNA was used in control and experimental conditions. In addition, however, some experiments were performed with higher mutant to wild-type  $Kv\alpha$ -subunit cDNA ratios (5:1; mutant to wild-type cDNAs) to assess the efficacy of the mutant constructs in attenuating wild-type  $K^+$  current amplitudes. In these experiments, the amount of carrier DNA (pSK) was reduced to maintain the total amount of DNA per 35 mm dish at 10  $\mu$ g.

**Isolation and in vitro maintenance of SCG neurons.** Sympathetic neurons were isolated from the SCGs of embryonic day 21 to postnatal day 1 Long-Evans rat pups using a procedure similar to that described previously by Chang et al. (1990). Briefly, after anesthesia with 5% halothane, animals were decapitated, and the SCGs were removed. Ganglia were successively incubated for 30 min periods in collagenase and trypsin at room temperature, and isolated SCG neurons were obtained by trituration and subsequent centrifugation. Dissociated SCG cells were resuspended in growth medium (EMEM with 10% FCS, 0.14 mM L-glutamine, 100 U/ml penicillin–streptomycin, and 0.05 mM NGF) and plated at a density of  $2.5 \times 10^4/cm^2$  on glial monolayers [prepared as described by Raff et al. (1979)]. Cells were maintained in a 95%  $O_2/5\%$   $CO_2$  37°C incubator, and the medium was exchanged with fresh growth medium approximately every 48 hr.

**Antibodies.** The monoclonal anti-Kv2.1 antibody used here was raised against residues 853–857 in the C terminus of Kv2.1 (Trimmer, 1991) and was obtained from Upstate Biochemicals, Inc. (Uppsala, NY). The

polyclonal Kv2.2-specific antibody, targeted against residues 771–788 in the C-terminal region of Kv2.2, was obtained from Dr. S. Trimmer (State University of New York, Stony Brook). A mouse monoclonal anti-FLAG antibody (Eastman Kodak, Rochester, NY) was used to detect Kv2.1W365C/Y380T-FLAG expression and a mouse monoclonal anti-myc antibody (Calbiochem, La Jolla, CA) was used to detect Kv2.2W373C/Y388T-*myc* in transfected SCG neurons. For immunohistochemistry, cells were fixed in 4% paraformaldehyde for 30 min, incubated in blocking buffer (PBS containing 5% normal goat serum, 0.02% Triton X-100, and 0.1%  $NaNH_3$ ) for 1 hr, and exposed to one of the Kv2  $\alpha$ -subunit-specific primary, anti-FLAG, or anti-MYC antibodies (1:500 dilution) at 4°C overnight. After washing with PBS, cultures were incubated either with a biotinylated goat anti-rabbit or donkey anti-mouse antibody (1:200 dilution; Chemicon) or with a Cy3-conjugated rabbit anti-mouse IgG secondary antibody (Chemicon) for 1 hr at room temperature. After wash, cultures were then exposed to avidin-conjugated horseradish peroxidase (HRP) for 1 hr at room temperature (ABC kit; Vector Laboratories, Burlingame, CA) or visualized directly under epifluorescence illumination. For detection of HRP, cultures were washed again before incubation with 0.05% diaminobenzidine in PBS. The progress of the reaction was monitored under the microscope, and the reactions were quenched after ~5 min by addition of PBS.

**Western blots.** Extracts of HEK-293 cells transfected with wild-type and mutant Kv2.x constructs and rat SCG (and brain) membrane preparations were prepared using methods described in detail previously (Barry et al., 1995; Pond et al., 2000). The protein content of each of the solubilized samples and the membrane preparations was determined using a Bio-Rad (Richmond, CA) protein assay kit with bovine serum albumin as the standard. For Western blot analysis, equal amounts of proteins were fractionated on 8–15% SDS-PAGE gels and transferred to polyvinylidene difluoride (PVDF) membranes (Bio-Rad). The PVDF membrane strips were incubated in 0.2% I-Block (Tropix) in PBS containing 0.1% Tween 20 (blocking buffer) for 1 hr at room temperature, followed by overnight incubation at 4°C with the monoclonal anti-Kv2.1 or the polyclonal anti-Kv2.2 antibody at dilutions of 1:500 or 1:100, respectively. After washing, membrane strips were incubated for 2 hr at room temperature with alkaline phosphatase-conjugated goat anti-rabbit or anti-mouse IgG (Tropix) diluted 1:5000 in the blocking buffer, and bound antibodies were detected using the CPSD chemiluminescent alkaline phosphatase substrate (Tropix).

**Immunoprecipitations.** For each immunoprecipitation experiment, the precipitating antibody (0.1  $\mu$ g) and 50  $\mu$ l of equilibrated protein-A Sepharose beads (Sigma) were added to 100  $\mu$ l of the HEK-293 or SCG (or brain) protein preparation (prepared as described above) and mixed (by inversion) at 4°C overnight. Eluted proteins were fractionated by SDS-PAGE, transferred to PVDF membranes, and immunoblotted with the monoclonal anti-Kv2.1 antibody or the polyclonal anti-Kv2.1 antibody as described above. After exposure to the appropriate (anti-mouse or anti-rabbit) secondary antibody, protein bands were visualized by enhanced chemiluminescence as described above.

**Transfection of isolated SCG neurons.** In control experiments, 1.6  $\mu$ m gold beads were coated with pCMV-EGFP (Clontech, Palo Alto, CA) and propelled (450 psi; 2 mm carrier distance) into SCG neurons at 4 d *in vitro* using the Biolistics Gene Gun (Bio-Rad). After transfections, the cultures appeared healthy, and expression of EGFP was readily detected 24 hr later. In experiments aimed at examining the effects of Kv2.1, Kv2.1W365C/Y380T, Kv2.2W373C/Y388T, or Kv2.1W365C/Y380T plus Kv2.2W373C/Y388T expression in SCG neurons, the gold particles were coated with pBK-CMV-Kv2.1 and pCMV-EGFP (4:1 ratio); pAlter-CMV-Kv2.1W365C/Y380T and pCMV-EGFP (4:1 ratio); pEF6/v5His-EF6-Kv2.2W373C/Y388T and pCMV-EGFP (4:1 ratio); or pAlter-CMV-Kv2.1W365C/Y380T, pEF6/v5His-EF6-Kv2.2W373C/Y388T, and pCMV-EGFP (2:2:1 ratio). In all cases, a total of 10  $\mu$ g of DNA was used in coating the beads. Because EGFP expression was used to identify transfected neurons for subsequent electrophysiological characterization, immunohistochemical experiments using the anti-FLAG and anti-MYC antibodies were also performed to determine whether EGFP-expressing cells also expressed the test constructs.

**Electrophysiological recording.** Whole-cell recordings were obtained from HEK-293 cells and from isolated SCG neurons 24–48 hr after transfection. Experiments were performed at room temperature (22–25°C), and data were collected using an Axopatch-1B patch-clamp amplifier interfaced to a P5-120 Gateway2000 computer through a Digidata 1200 and using the pClamp7 software package (Axon Instruments, Foster City, CA). Electrodes were fabricated from soda-lime glass (Chase

2502) with a two-stage puller, and the shanks were coated with a silicone elastomer (Sylgard; Dow Corning, Corning, NY). Pipette resistances were 1.5–3 M $\Omega$  after fire-polishing. For voltage-clamp recordings, the bath solution routinely contained (in mM): 140 NaCl, 4 KCl, 2 CaCl<sub>2</sub>, 2 MgCl<sub>2</sub>, 10 HEPES, 5 glucose, 0.001 TTX, and 0.1 CdCl<sub>2</sub>, pH 7.5, 300 mOsm. In current-clamp experiments on isolated SCG neurons, the TTX and CdCl<sub>2</sub> were omitted from the bath. The pipette solution for both current- and voltage-clamp recordings contained (in mM): 135 KCl, 10 HEPES, 5 glucose, 3 MgATP, 0.5 NaATP, 2 EGTA, and 1.1 CaCl<sub>2</sub>, pH 7.5, 300 mOsm. Series resistances, estimated from the decays of the uncompensated capacitive transients, were 2–5 M $\Omega$  and were compensated electronically by ~80–90%. Because current amplitudes were <10 nA, the voltage errors resulting from the uncompensated series resistance were always <10 mV and were not corrected.

In most experiments, voltage-gated K<sup>+</sup> currents were evoked during 125 msec or 6 sec depolarizing voltage steps to test potentials between –40 mV and +50 mV from a holding potential of –90 mV. To determine the activation profiles of the Kv2.1- and Kv2.2-encoded K<sup>+</sup> currents in HEK-293 cells and in rat SCG neurons under physiological conditions, experiments were also performed in which the voltage clamp was driven by average action potential waveform. Because SCG neurons display variable action potential waveforms and repetitive firing patterns (Malin and Nerbonne, 2000) and have been classified as phasic, tonic, and adapting, the activation profiles of the currents were examined in cells driven by each of these (action potential) phenotypes. In these experiments, action potentials recorded from representative phasic, tonic, and adapting cells were averaged and provided as the input to the voltage clamp. Outward K<sup>+</sup> currents recorded in Kv2.1- and Kv2.2-transfected HEK cells and in isolated rat SCG neurons in response to these action potential clamps were then recorded and analyzed. Single action potentials and action potential trains in isolated SCG neurons were recorded in response to brief (1.5 msec) 200–400 pA and prolonged (500 msec) 20–200 pA depolarizing current injections.

**Data analysis.** Data were compiled and analyzed using pClamp7 (Axon Instruments) and Excel (Microsoft, Redmond, WA) software and are presented as means  $\pm$  SEM. The decay phases of the capacitive transients were analyzed, and only cells in which >90% of the amplitude of the capacitive transient decayed over a single exponential time course were analyzed further. The mean  $\pm$  SEM input resistance and capacitance of EGFP-expressing SCG neurons were  $0.34 \pm 0.03$  G $\Omega$  and  $32 \pm 2$  pF ( $n = 43$ ), respectively. Leak currents were <10 pA (at –70 mV) and were not subtracted; leak conductances (at –70 mV) were always <0.15 nS. To determine the amplitudes and the decay time constants of the individual components of the total depolarization-activated outward K<sup>+</sup> currents in SCG neurons, the inactivation phases of the currents recorded during prolonged (6 sec) depolarizations were analyzed using the following equation:  $y = A_1 e^{-t/\tau_1} + A_2 e^{-t/\tau_2} + A_3 e^{-t/\tau_3} + C$ , where  $A_1$ ,  $A_2$ , and  $A_3$  (measured in picoamperes per picoFarad) are the amplitudes of the inactivating current components ( $I_{AB}$ ,  $I_{AS}$ , and  $I_K$ ) that decay with time constants  $\tau_1$ ,  $\tau_2$ , and  $\tau_3$  (measured in msec), respectively, and  $C$  is the steady-state current remaining at the end of the 6 sec depolarizations. Fits were obtained using Clampfit6, and best fits were determined by eye (in all cases,  $\sigma < 30$  pA). All current-clamp recordings were obtained from cells with overshooting action potentials and stable resting membrane potentials negative to –40 mV. Action potential durations (APDs) were measured at 50% (APD<sub>50</sub>) and 90% (APD<sub>90</sub>) repolarization. Statistical significance was examined with the Student's  $t$  test, and, where appropriate,  $p$  values are presented below.

## RESULTS

### Generation and characterization of dominant negative Kv2 $\alpha$ -subunits

In preliminary studies, a single point mutation was introduced into the pore region of Kv2.1, analogous to the approaches used to generate the dominant negative Kv4.2  $\alpha$ -subunit, Kv4.2W362F (Barry et al., 1998), and the dominant negative Kv1.5  $\alpha$ -subunit, Kv1.5W461F (Li et al., 1999). However, heterologous expression studies revealed that this construct produced outward K<sup>+</sup> currents indistinguishable from those evident on expression of wild-type (rat) Kv2.1. These results are similar to those described by Blaine and Ribera (1998) in studies with *Xenopus* Kv2.2. Because a functional dominant negative construct was obtained by intro-

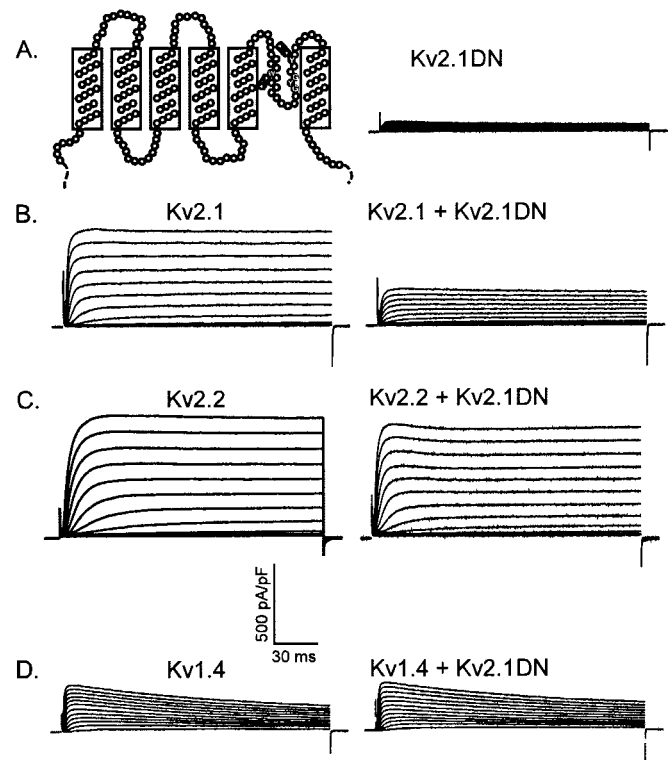


**Figure 1.** Kv2.1W365C/Y380T (Kv2.1DN) specifically attenuates Kv2.1-encoded currents in HEK cells. Whole-cell voltage-gated outward K<sup>+</sup> currents were recorded from HEK-293 cells expressing Kv2.1DN alone (*A*), Kv2.1 or Kv2.1 plus Kv2.1DN (*B*), Kv2.2 or Kv2.2 plus Kv2.1DN (*C*), Kv1.4 or Kv1.4 plus Kv2.1DN (*D*), and EGFP. Cells were transfected with cDNA constructs (1:1) encoding these subunits, and currents were obtained from EGFP-positive cells as described in Materials and Methods. Schematic of Kv2.1DN is shown, with altered residues. *A*, In cells expressing Kv2.1DN alone, outward K<sup>+</sup> currents are indistinguishable from those in wild-type HEK-293 cells. *B*, In HEK-293 cells coexpressing Kv2.1DN and Kv2.1, current densities are reduced markedly compared with those recorded from cells expressing Kv2.1 alone (compare *left* and *right*). *C*, In contrast, coexpression of Kv2.1DN with Kv2.2 reveals outward currents indistinguishable from those measured in cells expressing Kv2.2 alone. *D*, Outward K<sup>+</sup> currents in cells expressing Kv2.1DN and Kv1.4 are indistinguishable from those expressing Kv1.4 alone.

ducing two mutations in the pore region of *Xenopus* Kv2.2 (Blaine and Ribera, 1998), a similar strategy was used here for (rat) Kv2.1 to generate a double pore mutant, Kv2.1W365C/Y380T (see Materials and Methods). The Kv2.1W365C/Y380T construct, Kv2.1DN, was epitope-tagged at the C terminus with the 8 aa FLAG tag to allow direct detection of transgene expression.

To determine the functional properties of this construct, HEK-293 cells were transfected with Kv2.1DN (and EGFP) alone and in combination with Kv2.1, Kv2.2, or Kv1.4 (in a 1:1 ratio; see Materials and Methods), and outward K<sup>+</sup> currents, evoked in response to 125 msec depolarizing voltage steps to potentials ranging from –40 mV to +50 mV from a holding potential of –70 mV, were recorded (Fig. 1). These experiments revealed that mean  $\pm$  SEM peak outward K<sup>+</sup> current densities ( $30 \pm 7$  pA/pF;  $n = 9$ ) in HEK-293 cells expressing Kv2.1DN alone (Fig. 1*A*) are not significantly different from those recorded from wild-type or mock-transfected HEK-293 cells ( $15 \pm 6$  pA/pF;  $n = 11$ ). However, when the Kv2.1DN is coexpressed with wild-type Kv2.1, outward K<sup>+</sup> currents are attenuated markedly compared with those recorded from cells expressing Kv2.1 (and EGFP) alone

**Table 1. Subunit-specific assembly of Kv2.1DN and Kv2.2DN in HEK-293 cells<sup>a</sup>**

	Kv2.1	Kv2.2	Kv1.4
Alone	361 ± 53 <i>n</i> = 25	529 ± 49 <i>n</i> = 32	299 ± 58 <i>n</i> = 12
Plus Kv2.1DN	148 ± 19* <i>n</i> = 40	536 ± 38 <i>n</i> = 41	339 ± 53 <i>n</i> = 14
Plus Kv2.2DN	370 ± 32 <i>n</i> = 27	298 ± 36* <i>n</i> = 25	

<sup>a</sup>Mean ± SEM current densities (in picoamperes per picoFarad) at +50 mV are reported.

\*Values are significantly ( $p < 0.001$ ) different from those measured in cells expressing wild-type Kv2.1 or Kv2.2 alone.

(Fig. 1*B*, Table 1). Although current amplitudes are attenuated markedly, the time- and voltage-dependent properties of the residual currents are indistinguishable from those determined in cells expressing Kv2.1 alone. Increasing the relative amount of the Kv2.1DN to wild-type Kv2.1 to 5:1 completely eliminated the Kv2.1-encoded  $K^+$  currents. Unexpectedly, however, the currents produced on coexpression of Kv2.1DN with Kv2.2 in a 1:1 ratio are indistinguishable from those produced by Kv2.2 alone (Fig. 1*C*, Table 1). Similar results were obtained when the (1:1) ratio of the mutant construct Kv2.1DN to wild-type Kv2.2 was increased to 5:1. Immunohistochemical experiments with the anti-FLAG antibody (see Materials and Methods) revealed that the expression levels of the Kv2.1DN protein were similar in HEK-293 cells expressing Kv2.1 or Kv2.2 (data not shown). Together, these results suggest that, in HEK-293 cells, Kv2.1DN does not assemble with Kv2.2 (see also below). Additional experiments revealed that coexpression of Kv2.1DN does not measurably affect the currents produced on expression of Kv1.4 (Fig. 1*D*, Table 1) or other  $Kv\alpha$ -subunits (data not shown), revealing that the Kv2.1DN construct selectively coassembles with Kv2.1.

A similar strategy was exploited to generate a double pore mutant of Kv2.2, Kv2.2W373C/Y388T, that also functions as a dominant negative (Kv2.2DN); this construct was *myc* epitope-tagged at the C terminus (see Materials and Methods). Electrophysiological experiments revealed that mean ± SEM peak outward  $K^+$  current densities ( $26 \pm 6$  pA/pF;  $n = 10$ ) recorded from HEK-293 cells expressing Kv2.2DN (Fig. 2*A*) are not significantly different from those recorded from wild-type or mock-transfected HEK-293 cells ( $15 \pm 6$  pA/pF;  $n = 11$ ). However, coexpression of Kv2.2DN with wild-type Kv2.2 (1:1) markedly reduced peak outward  $K^+$  current densities compared with the currents recorded from cells expressing Kv2.2 (and EGFP) alone (Fig. 2*B*, Table 1). The time- and voltage-dependent properties of the residual currents are indistinguishable from those determined in HEK-293 cells expressing Kv2.2 alone. Increasing the relative amount of the Kv2.2DN to wild-type Kv2.2 cDNA to 5:1 eliminated the Kv2.2-encoded  $K^+$  currents. Similar to the findings with Kv2.1DN and Kv2.2 (Fig. 1*C*), coexpression of Kv2.2DN with wild-type Kv2.1 at a 1:1 (Fig. 2*C*, Table 1) or 5:1 ratio does not measurably affect Kv2.1-encoded currents. Immunohistochemical experiments with the anti-*myc* antibody revealed that the expression levels of the Kv2.2DN-*myc*, however, are similar in Kv2.2- and Kv2.1-expressing HEK-293 cells (data not shown). Therefore, these combined observations are consistent with the hypothesis advanced above that Kv2.1 and Kv2.2 do not coassemble in HEK-293 cells (see also below).

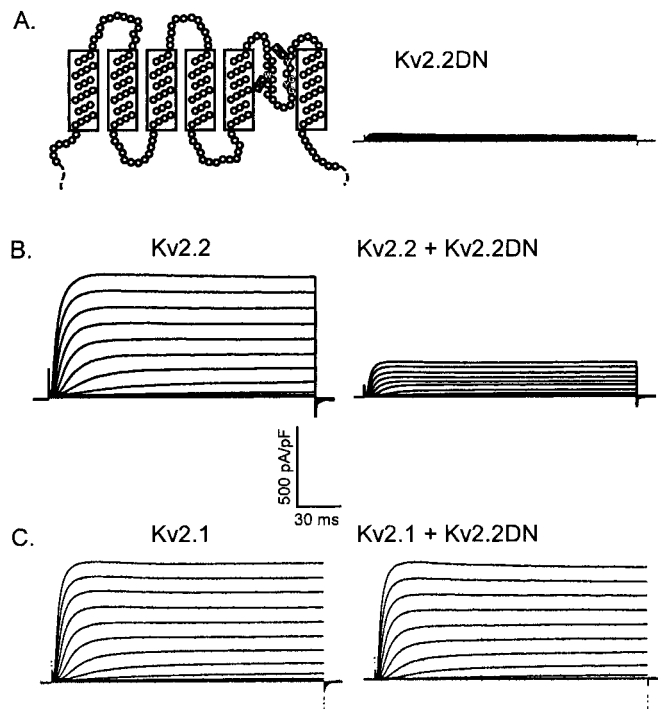


**Figure 2.** Kv2.2W373C/Y388T (Kv2.2DN) specifically attenuates Kv2.2-encoded currents in HEK cells. Whole-cell voltage-gated outward  $K^+$  currents were recorded from HEK-293 cells expressing Kv2.2DN (*A*), Kv2.2 or Kv2.2 plus Kv2.2DN (*B*), Kv2.1 or Kv2.1 plus Kv2.2DN (*C*), and EGFP, as described in the legend to Figure 1. *A*, Schematic of Kv2.2DN is shown, with the altered residues indicated. In cells expressing Kv2.2DN alone, outward  $K^+$  currents are similar to those in wild-type cells. *B*, When Kv2.2DN is coexpressed with Kv2.2, however, Kv2.2-encoded outward  $K^+$  currents are reduced compared with cells expressing Kv2.2 alone (compare *left* and *right*). *C*, In contrast, Kv2.2DN does not affect Kv2.1-encoded currents.

### Expression of Kv2.1DN or Kv2.2DN attenuates $I_K$ in SCG neurons

To assess the functional consequences of expression of the Kv2.x dominant negative constructs on outward  $K^+$  currents in SCG neurons, cells were transfected with Kv2.1DN-FLAG or Kv2.2DN-*myc* (and EGFP) using the Biolistics Gene Gun (see Materials and Methods). As reported previously (Malin and Nerbonne, 2000, 2001) EGFP is readily detected in the cell bodies of SCG cells within ~15 hr of transfection (data not shown). Cells were stained with the anti-FLAG or anti-*myc* antibody to verify expression of the transgenes, Kv2.1DN and Kv2.2DN, and both constructs were readily detected in all EGFP-positive cells (data not shown). Also similar to previous findings using this methodology (Malin and Nerbonne, 2000, 2001), all EGFP-positive cells in these cultures also expressed the transgene.

Representative whole-cell voltage-gated outward  $K^+$  currents recorded from three EGFP-positive Kv2.1DN-expressing SCG cells are presented in Figure 3 (*middle*). As in wild-type cells (Fig. 3, *left*), type I, type II, and type III Kv2.1DN-expressing cells were readily distinguished (Table 2). Most (~70%) cells express  $I_{AF}$ ,  $I_K$ , and  $I_{SS}$ , and are therefore classified as type I cells (Malin and Nerbonne, 2000). However, the density of  $I_K$  in Kv2.1DN-expressing type I cells is significantly ( $p < 0.005$ ) lower than  $I_K$  density in wild-type I cells (Table 2). Approximately 20% of the Kv2.1DN-expressing SCG cells are type II (expressing  $I_{AF}$ ,  $I_{AS}$ ,  $I_K$ , and  $I_{SS}$ ), similar to the percentage (~25%) of wild-type II cells

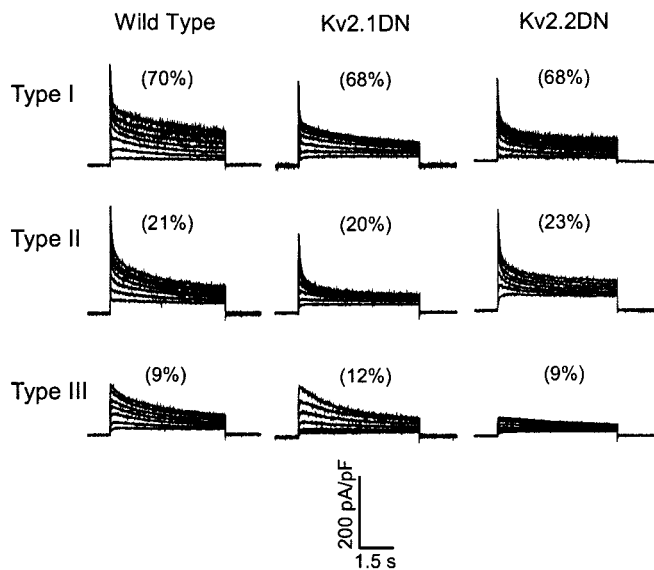


**Figure 3.** Expression of Kv2.1DN or Kv2.2DN reduces  $I_K$  density in SCG neurons. Whole-cell voltage-gated outward  $K^+$  currents were recorded from isolated SCG neurons in response to 6 sec depolarizing voltage steps to test potentials between  $-10$  and  $+50$  mV from a holding potential of  $-90$  mV. Experiments were conducted as described in Materials and Methods, with  $1 \mu\text{M}$  TTX and  $100 \mu\text{M}$  CdCl<sub>2</sub> in the bath solution to block voltage-gated inward  $\text{Na}^+$  and  $\text{Ca}^{2+}$  currents, respectively. The records shown to the left, middle, and right were recorded from wild-type, Kv2.1DN-expressing, and Kv2.2DN-expressing cells, respectively. There are distinct and stereotyped differences in the waveforms of the currents in wild-type I, type II, and type III SCG cells (Malin and Nerbonne, 2000). The numbers given above the records in each column reflect the percentages of cells studied under each experimental condition that display the type I, type II, or type III outward  $K^+$  current phenotype. Although the percentages of type I, type II, and type III Kv2.1DN- or Kv2.2DN-expressing cells are not different from those in wild-type SCG cells, expression of either Kv2.1DN (middle) or Kv2.2DN (right) decreases the density of the slowly decaying current,  $I_K$ , in type I cells. Expression of Kv2.1DN also decreases  $I_K$  density in type II cells (middle).

(Fig. 3, Table 2). In type II, as in type I, cells, Kv2.1DN expression significantly ( $p < 0.05$ ) reduces  $I_K$  density (Table 2). In both type I and type II cells, the effects of Kv2.1DN expression are specific; neither the densities of  $I_{Af}$ ,  $I_{As}$ , or  $I_{SS}$  nor the kinetics of  $I_{Af}$  or  $I_{As}$  decay in these cells are significantly different from those measured in wild-type I and II SCG cells (Table 2). Similar to the findings in wild-type cells,  $\sim 10\%$  of Kv2.1DN-expressing cells are classified as type III SCG neurons, expressing only  $I_K$  and  $I_{SS}$ , and, interestingly,  $I_K$  density in type III cells is unaffected by Kv2.1DN expression (Table 2). Therefore, expression of Kv2.1DN results in the selective attenuation (by  $\sim 50\%$ ) of  $I_K$  in type I and type II SCG cells.

Similar experiments were conducted on cells expressing Kv2.2DN, and representative outward  $K^+$  currents recorded from (3) Kv2.2DN- (and EGFP) expressing SCG neurons are shown in Figure 3 (right). As in wild-type and Kv2.1DN-expressing SCG cells, most ( $\sim 70\%$ ) Kv2.2DN-expressing cells can be classified as type I, expressing  $I_{Af}$ ,  $I_{As}$ ,  $I_K$ , and  $I_{SS}$ . In Kv2.2DN-expressing type I cells (Fig. 3),  $I_K$  density is significantly ( $p < 0.005$ ) lower than in wild-type I SCG neurons (Table 2). The densities of  $I_{Af}$  and  $I_{SS}$  and the kinetics of  $I_{Af}$  and  $I_K$  decay, in contrast, are unaffected by Kv2.2DN expression (Table 2). In  $\sim 20\%$  of the Kv2.2DN-expressing SCG cells,  $I_{Af}$ ,  $I_{As}$ ,  $I_K$ , and  $I_{SS}$  were evident, and these cells were classified as type II (Malin and Nerbonne, 2000). The mean  $\pm$  SEM densities and inactivation

rates of  $I_{Af}$ ,  $I_{As}$ ,  $I_K$ , and  $I_{SS}$  in Kv2.2DN-expressing type II cells are not significantly different from those recorded in wild-type II cells (Table 2). In contrast to the findings with Kv2.1DN, which reduces  $I_K$  density in type I and type II cells, expression of Kv2.2DN reduces  $I_K$  density in type I cells without affecting  $I_K$  density in type II cells (Table 2). In these experiments, two Kv2.2DN-expressing cells were classified as type III cells (expressing  $I_K$  and  $I_{SS}$ ). Although  $I_K$  densities in these (2) cells are lower than in wild-type III cells (Table 2), the small number of Kv2.2DN-expressing type III cells precluded statistical analysis.

### Coexpression of Kv2.1DN and Kv2.2DN eliminates most of $I_K$ in SCG neurons

The results of the experiments described above suggested that the Kv2.1 and Kv2.2  $\alpha$ -subunits form distinct populations of  $I_K$  channels in SCG cells, and that Kv2.1-encoded  $I_K$  channels are expressed in both type I and type II cells, whereas Kv 2.2-encoded  $I_K$  channels are expressed only in type I SCG cells (Table 2). To explore this hypothesis further, currents were recorded from cells expressing both Kv2.1DN and Kv2.2DN (and EGFP). In these experiments, the relative amounts of the Kv2.1DN and Kv2.2DN cDNAs were the same, and each was one-half of the amounts of each used in the single transfection experiments (Fig. 3) to avoid any possible complications attributable to gene dosage effects. As is evident in the records shown in Figure 4, the combined expression of Kv2.1DN and Kv2.2DN eliminates  $I_K$  in most cells. In 12 of 16 (75%) of the cells examined, only  $I_{Af}$  and  $I_{SS}$  were detected; these cells were classified as type I cells lacking  $I_K$  (Table 2). The remaining four (of 16; 25%) cells are classified as type II cells, expressing  $I_{Af}$ ,  $I_{As}$ ,  $I_K$ , and  $I_{SS}$ , although the mean  $\pm$  SEM  $I_K$  density is reduced markedly in these cells, compared with wild-type II cells (Table 2). However, the mean  $\pm$  SEM  $I_K$  density in type II cells expressing both Kv2.1DN and Kv2.2DN is not significantly different from the  $I_K$  density in Kv2.1DN-expressing cells, consistent with the hypothesis that Kv2.1 but not Kv2.2 contributes to  $I_K$  in type II cells. Importantly, in both type I and type II cells,  $I_{Af}$ ,  $I_{As}$ , and  $I_{SS}$  are unaffected by the combined expression of Kv2.1DN and Kv2.2DN, indicating that Kv2  $\alpha$ -subunits do not contribute to these currents (Table 2). In these experiments, no type III cells (expressing  $I_K$  and  $I_{SS}$ ) were detected, an observation that likely reflects the small number (16) of cells studied.

### Expression of Kv2 $\alpha$ -subunits in rat SCG neurons

Together, the simplest interpretation of the results presented above is that Kv2.1- and Kv2.2-encoded  $K^+$  channels underlie  $I_K$  in type I cells, whereas only Kv2.1 (and not Kv2.2) channels contribute to  $I_K$  in type II cells. These findings suggest that there is an additional component of  $I_K$  in type II SCG neurons that is not encoded by Kv2  $\alpha$ -subunits. In addition, the combined observations in Kv2.1DN-, Kv2.2DN-, and Kv2.1DN plus Kv2.2DN-expressing SCG cells suggest that the Kv2.1 and Kv2.2  $\alpha$ -subunits do not associate to form heteromultimeric  $K^+$  channels in SCG neurons. Therefore, these results are consistent with the electrophysiological findings in HEK-293 cells suggesting that Kv2.1 and Kv2.2 do not coassemble (Figs. 1, 2). Consequently, subsequent experiments were focused on examining Kv2.1 and Kv2.2 expression in HEK-293 cells and in SCG neurons and on determining whether Kv2.1 and Kv2.2 are associated *in situ*.

Biochemical experiments were performed on extracts of Kv2.1 and Kv2.2-transfected HEK-293 cells and on fractionated SCG neuronal membranes using specific anti-Kv2.1 and anti-Kv2.2

**Table 2.** Expression of Kv2.1DN or Kv2.2DN attenuates  $I_K$  in SCG neurons<sup>a</sup>

Phenotype	Wild type <sup>b</sup>			Kv2.1DN			Kv2.2DN			Kv2.1DN plus Kv2.2DN	
	Type I	Type II	Type III	Type I	Type II	Type III	Type I	Type II	Type III	Type I	Type II
Peak current density (pA/pF)	252 ± 20	259 ± 22	211 ± 18	197 ± 17	207 ± 23	223 ± 16	185 ± 13*	227 ± 19	79	137 ± 17**	230 ± 24
$I_{Af}$ density (pA/pF)	81 ± 11	111 ± 21		82 ± 4	98 ± 13		69 ± 4	88 ± 10		73 ± 6	102 ± 19
$\tau$ (msec)	121 ± 14	95 ± 8		131 ± 5	122 ± 11		122 ± 12	92 ± 6		128 ± 18	97 ± 8
$I_{As}$ density (pA/pF)		45 ± 3			33 ± 3			46 ± 5			43 ± 7
$\tau$ (msec)		480 ± 21			542 ± 31			430 ± 39			571 ± 44
$I_K$ density (pA/pF)	108 ± 12	64 ± 9	136 ± 11	60 ± 2**	35 ± 4*	136 ± 8	41 ± 6**	49 ± 3	44		24 ± 3*
$\tau$ (msec)	2560 ± 167	2800 ± 193	2200 ± 176	2300 ± 183	3245 ± 525	1798 ± 203	3008 ± 310	3293 ± 438	2889		3438 ± 417
$I_{SS}$ density (pA/pF)	74 ± 5	45 ± 5	79 ± 6	59 ± 2	40 ± 4	80 ± 11	67 ± 3	44 ± 6	35	72 ± 6	59 ± 17
<i>n</i>	30	9	4	17	5	3	15	5	2	12	4

<sup>a</sup>All values are mean ± SEM; current densities and  $\tau_{\text{decay}}$  values were determined from currents recorded on depolarizations to +50 mV; *n* = number of cells.

<sup>b</sup>Data from Malin and Nerbonne (2000).

\*\*Values in Kv2.1DN- and Kv2.2DN-expressing cells are significantly (\*\**p* < 0.005; \**p* < 0.05) different from those recorded in wild-type cells.

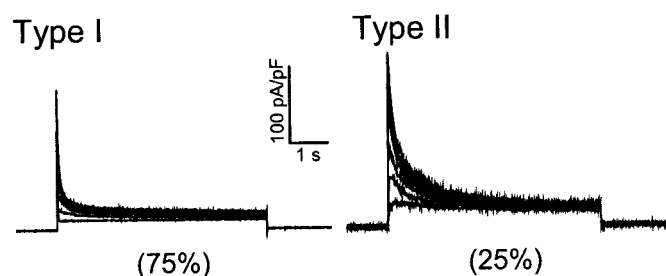


**Figure 4.** Coexpression of Kv2.1DN and Kv2.2DN eliminates  $I_K$  in most SCG neurons. Isolated SCG neurons were transfected with both Kv2.1DN and Kv2.2DN (and EGFP) using the Biolistics Gene Gun (as described in Materials and Methods), and outward  $K^+$  currents were recorded from EGFP-positive cells as described in the legend to Figure 3. Two distinct current waveforms were evident in these recordings: most (75%) cells were found to express only  $I_{Af}$  and  $I_{SS}$  and therefore are type I cells lacking  $I_K$ ; the remaining cells (25%) express  $I_{Af}$ ,  $I_{As}$ ,  $I_K$ , and  $I_{SS}$  and are classified as type II cells with reduced  $I_K$  density (Table 2). The densities of  $I_{Af}$ ,  $I_{As}$ , and  $I_{SS}$  in Kv2.1DN plus Kv2.2DN-expressing type I and type II cells are indistinguishable from those measured in wild-type I and II cells (Table 2).

antibodies (see Materials and Methods). As illustrated in Figure 5A, the anti-Kv2.1 antibody detects a single band at ~114 kDa in HEK-293 cells transfected with Kv2.1 and Kv2.2. Similarly, in blots probed using the anti-Kv2.2 antibody, a single protein band at ~90 kDa was identified (Fig. 5A). Western blot analysis also revealed robust expression of Kv2.1 and Kv2.2 in lysates of rat SCG (Fig. 5A). Importantly, both the anti-Kv2.1 and the anti-Kv2.2 antibodies can be used to immunoprecipitate proteins (against which each of these antibodies was targeted) from homogenates of HEK-293 cells transfected with both the Kv2.1 and Kv2.2 cDNAs (Fig. 5B). In contrast, however, Kv2.2 does not coimmunoprecipitate with the anti-Kv2.1 antibody, and Kv2.1 does not precipitate with the anti-Kv2.2 antibody (Fig. 5B). When the immunoprecipitation was performed with the anti-Kv2.1 antibody, the Kv2.2 (nonprecipitating) protein was identified in the supernatant (Fig. 5B, lanes S). In addition, when the anti-Kv2.2 antibody was used in the immunoprecipitation, the Kv2.1 (nonprecipitating) protein was readily detected in the supernatants (Fig. 5B, lanes S). Similar results were obtained in experiments performed on lysates of rat SCG. The anti-Kv2.1 antibody precipitates the Kv2.1 protein but not the Kv2.2 protein expressed in SCG neurons (Fig. 5C). Similarly, after immunoprecipitations

with the anti-Kv2.2 antibody, the Kv2.2 protein is found in the pellet (Fig. 5C, lane P), whereas the Kv2.1 protein is in the supernatant (Fig. 5C, lane S). Together, these data suggest that Kv2.1 and Kv2.2 do not associate either in HEK-293 cells or in SCG neurons but rather preferentially form monomeric (Kv2.1 or Kv2.2) voltage-gated  $K^+$  channels.

#### Kv2.1-encoded $I_K$ channels regulate action potential durations in tonic SCG cells

In wild-type rat SCG neurons, three distinct repetitive firing patterns, phasic, adapting, and tonic, are observed in response to prolonged (6 sec) depolarizing current injections (Malin and Nerbonne, 2000). These studies revealed that ~45% of the cells are phasic, firing one or two action potentials, and then become refractory in response to prolonged (6 sec) current injections. Importantly, phasic cells do not fire additional action potentials in response to larger current injections. In contrast, adapting cells (~30%) fire trains of action potentials in response to low amplitude current injections. However, when the amplitude of the current injection is increased, the firing rate adapts and these cells become refractory. Adapting cells were further distinguished (from phasic and tonic cells) by increased input resistances and decreased current thresholds for action potential generation. Approximately 25% of wild-type SCG cells fire trains of action potentials in response to depolarizing current injections, and the firing frequency increases with the amplitude of the injected current [i.e., no refractoriness is evident in these (tonic) cells over the range of injected currents examined]. Tonic cells were also distinguished from phasic and adapting cells by briefer action potential durations (Malin and Nerbonne, 2000).

In initial experiments focused on exploring the hypothesis that Kv2.x-encoded  $I_K$  channels might play a role in shaping action potential waveforms in SCG neurons, Kv2.x-expressing HEK-293 cells and isolated SCG neurons were held at -48 mV (the mean resting membrane potential of rat SCG neurons), and a voltage-clamp paradigm that simulates action potentials typically recorded in phasic, adapting, and tonic SCG neurons was presented. The action potential clamp paradigms are illustrated in Figure 6 (bottom). As illustrated at the top of Figure 6, Kv2.1-encoded  $K^+$  currents in HEK-293 cells are activated similarly using the phasic, tonic, and adapting action potential clamp waveforms. The outward  $K^+$  currents peak ~1 msec after the peak of the action potential at current densities of ~25–40 pA/pF (Table 3). This is ~20% of the current activated in these cells by a step depolar-

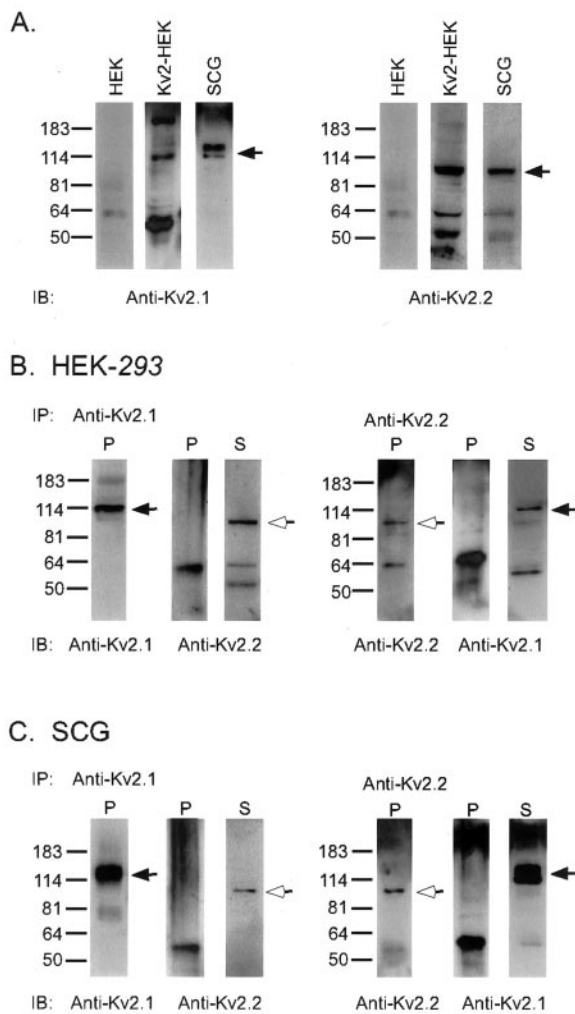


**Figure 5.** Kv2.1 and Kv2.2 are expressed in rat SCGs but do not appear to associate. *A*, Lysates of control and transfected HEK-293 cells and of isolated rat SCGs were fractionated in SDS-PAGE gels and immunoblotted (IB) with the monoclonal anti-Kv2.1 (left) and the polyclonal anti-Kv2.2 (right) antibodies. *B*, *C*, Lysates prepared from transfected HEK-293 cells (*B*) and rat SCG neurons (*C*) were immunoprecipitated (IP) with either the monoclonal anti-Kv2.1 or the polyclonal anti-Kv2.2 antibody, fractionated, and immunoblotted with the same antibodies. Although both the anti-Kv2.1 and anti-Kv2.2 antibodies reliably immunoprecipitate the proteins against which each of these antibodies were generated, the Kv2.1 and Kv2.2  $\alpha$ -subunits do not coimmunoprecipitate from lysates prepared from Kv2.1- and Kv2.2-transfected HEK-293 cells or rat SCGs. After immunoprecipitations with the anti-Kv2.1 antibody, the Kv2.2 protein is evident in the supernatants (lanes *S*) but not in the pellet (lanes *P*). Similarly, the Kv2.1 protein is found in the supernatant (*S*) after immunoprecipitation with the anti-Kv2.2 antibody. Closed arrows indicate Kv2.1; open arrows indicate Kv2.2.

ization to +50 mV ( $289 \pm 60$  pA/pF; see Table 1). Therefore, substantial currents can be evoked by single neuronal action potential waveforms when Kv2.x subunits are expressed in HEK-293 cells. These findings are consistent with the results observed using standard voltage-step protocols, which reveal activation thresholds between  $-40$  mV and  $-30$  mV for Kv2.x channels in HEK cells (Figs. 1, 2).

To probe directly the activation of Kv2.x channels in SCG cells, similar experiments were performed in SCG cells using the action potential clamp paradigms (Fig. 6). Peak outward  $K^+$  current densities measured in SCG cells with the action potential clamp

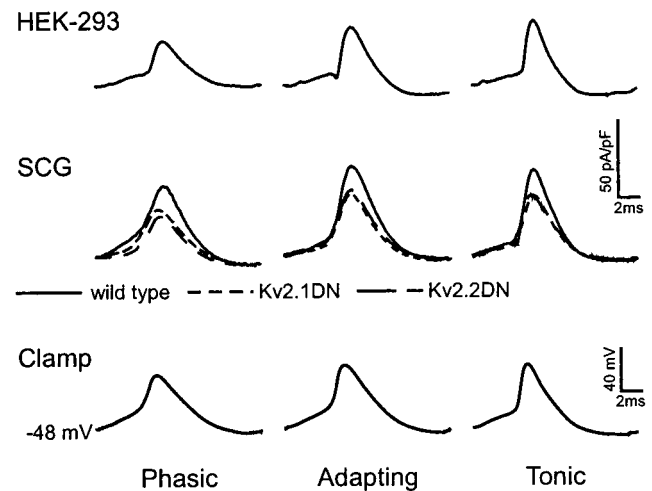


**Figure 6.** Activation of Kv2-encoded  $K^+$  currents during action potentials in SCG neurons. To explore directly the activation of Kv2.x-encoded  $K^+$  currents during action potential waveforms in SCG neurons, cells were held at the typical resting membrane potential of SCG neurons ( $\sim -48$  mV; see Table 3), and outward  $K^+$  currents activated by typical phasic, adapting, and tonic action potential waveforms were recorded. The voltage-clamp paradigms are illustrated at the bottom. Representative outward current waveforms in Kv2.1-expressing HEK-293 cells driven by the phasic adapting and tonic action potential waveforms are illustrated at the top. Representative outward  $K^+$  current waveforms in isolated SCG neurons (activated using the action potential voltage-clamp paradigms shown below the record) are presented at the bottom. Action potential clamp recordings from wild-type (solid line), Kv2.1DN-expressing (short dashed line), and Kv2.2DN-expressing (long dashed line) SCG cells are superimposed for comparison purposes.

paradigm are  $50$ – $60$  pA/pF (Table 3). Comparison of these values with current densities measured using the conventional step depolarization paradigm (Fig. 3) reveals that peak current densities activated during the action potential clamp are  $\sim 25\%$  of the mean peak current densities measured at  $+50$  mV in response to step depolarizations from  $-70$  mV (Fig. 3, Table 2). In addition, in SCG cells expressing Kv2.1DN or Kv2.2DN, peak outward  $K^+$  currents activated by phasic, tonic, and adapting action potential clamp waveforms are reduced significantly compared with those in wild-type cells (Table 3). Representative voltage-clamp records are illustrated in the middle of Figure 6. As might be expected from the data in HEK-293 cells, these analyses suggest that the contribution of the Kv2.x-encoded  $K^+$  currents is greater at the time corresponding to 50% rather than 90% repolarization. Together, these observations suggest that there is substantial outward  $K^+$  current through Kv2-encoded  $K^+$  channels in SCG neurons during action potentials, and also that blocking Kv2-encoded  $K^+$  currents likely would impact action potential durations. Subsequent experiments were aimed at testing this hypothesis directly.

The phasic, adapting, and tonic firing patterns seen in wild-type SCG cells are also evident in recordings from cells expressing Kv2.1DN, and the selective attenuation of the Kv2.1-encoded  $I_K$  does not affect the distribution of firing patterns (Fig. 7). The expression of Kv2.1DN also does not affect the mean  $\pm$  SEM input resistances, resting potentials, action potential amplitudes, or the current thresholds for action potential generation in phasic, adapting, or tonic SCG cells (Table 4). As in wild-type SCG cells, Kv2.1DN-expressing adapting cells are readily distinguished from phasic and tonic cells by increased input resistances and lower

**Table 3. Contribution of Kv2.1- and Kv2.2-encoded  $I_K$  to action potential repolarization<sup>a</sup>**

	Peak current density	Current density at APD <sub>50</sub>	Current density at APD <sub>90</sub>	<i>n</i>
HEK-293 Tf Kv2.1				
Phasic	27 ± 3	21 ± 2	10 ± 3	10
Adapting	38 ± 3	33 ± 3	14 ± 3	
Tonic	39 ± 4	32 ± 4	16 ± 3	
HEK-293 Tf Kv2.2				
Phasic	23 ± 3	18 ± 3	9 ± 2	11
Adapting	28 ± 4	23 ± 5	12 ± 3	
Tonic	33 ± 4	27 ± 5	12 ± 3	
SCG wild type				
Phasic	52 ± 2	38 ± 1	10 ± 1	21
Adapting	60 ± 3	46 ± 2	10 ± 1	
Tonic	59 ± 3	50 ± 3	11 ± 1	
SCG Tf Kv2.1DN				
Phasic	30 ± 2**	22 ± 1**	7 ± 1**	18
Adapting	42 ± 1**	33 ± 2**	10 ± 1	
Tonic	42 ± 2**	35 ± 2**	7 ± 1*	
SCG Tf Kv2.2DN				
Phasic	35 ± 2**	24 ± 1**	6 ± 1**	17
Adapting	44 ± 2**	33 ± 2**	9 ± 1	
Tonic	43 ± 3**	34 ± 2**	6 ± 1*	

<sup>a</sup>All values (in picoamperes per picoFarad) are means ± SEM of data obtained from cells stimulated with an average phasic, adapting, or tonic action potential waveform.

\*\*\*Mean values are significantly different from those in wild-type SCG cells at the \**p* < 0.01 and \*\**p* < 0.002 levels.

current thresholds for action potential generation (Table 4). In tonic cells expressing the Kv2.1DN, however, the mean ± SEM action potential duration at 90% repolarization is significantly (*p* < 0.02) longer than in wild-type tonic cells (Fig. 7*B*, Table 4). Interestingly, although action potential durations in Kv2.1DN-expressing tonic cells are prolonged, tonic firing is not eliminated, and the firing frequencies of tonic cells are unchanged. Therefore, brief action potentials, regulated by Kv2.1-encoded  $I_K$ , are not the sole determinant of tonic firing.

#### Kv2.2-encoded $I_K$ channels regulate action potential threshold and repolarization

To explore the functional role of Kv2.2-encoded  $I_K$  channels, current-clamp recordings were obtained from SCG cells expressing Kv2.2DN (and EGFP). Similar to the findings with Kv2.1DN, all three firing patterns are observed in Kv2.2DN-expressing cells (Fig. 8). Also, similar to the findings with Kv2.1DN, action potential durations at 90% repolarization in tonic cells expressing Kv2.2 are significantly (*p* < 0.02) longer than in tonic wild-type cells (Table 4). However, in contrast to the findings with Kv2.1DN, expression of Kv2.2DN results in an increase in the percentage of adapting cells and a decrease in the percentage of phasic cells (Fig. 8, Table 4). Elimination of Kv2.2-encoded  $I_K$  channels also has marked effects on the excitability of SCG neurons. In adapting and tonic cells expressing Kv2.2DN, for example, resting membrane potentials are depolarized significantly (*p* < 0.001) compared with resting membrane potentials in wild-type adapting and tonic SCG cells (Table 4). In addition, the current thresholds for action potential generation are reduced significantly in phasic (*p* < 0.002) and in tonic (*p* < 0.02) firing

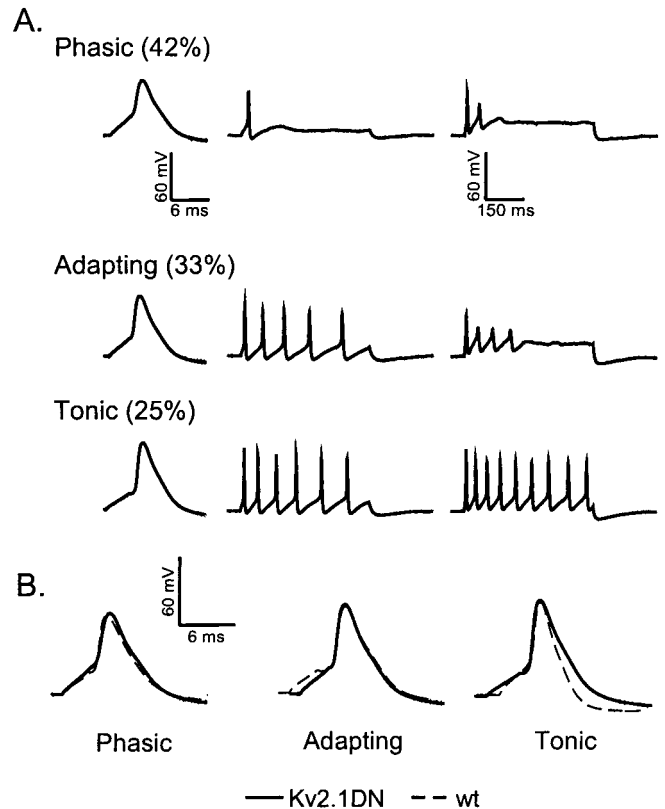


**Figure 7.** Phasic, adapting, and tonic firing patterns in SCG neurons expressing Kv2.1DN. SCG neurons were transfected with Kv2.1DN (and EGFP), and action potentials and repetitive firing patterns were recorded in response to brief or prolonged depolarizing current injections, as described in Materials and Methods. *A*, Current-clamp recordings from three representative Kv2.1DN-expressing cells are shown. In each cell, single action potentials were elicited by 1.5 msec current injections (*left*), and repetitive firing patterns were recorded in response to 100 pA (*middle*) or 200 pA (*right*) 500 msec current injections. Based on the response(s) to the 500 msec current injections, cells were classified as phasic (*top*), adapting (*middle*), or tonic (*bottom*) (Table 4). Although Kv2.1DN expression does not affect the distribution of firing patterns in SCG neurons, action potentials in tonic cells expressing Kv2.1DN are prolonged (*B*). Action potential durations in phasic and adapting cells (*B*), in contrast, are unaffected by Kv2.1DN expression (Table 4). *wt*, Wild type.

SCG cells expressing Kv2.2DN. However, input resistances and action potential amplitude are unaffected by Kv2.2DN expression (Table 4). Together, these results suggest that, unlike Kv2.1-encoded  $I_K$  channels, Kv2.2-encoded  $I_K$  channels play a role in setting resting potentials and in regulating action potential generation.

#### Elimination of $I_K$ prolongs action potentials and reduces tonic firing

The voltage-clamp experiments detailed above revealed that expression of either Kv2.1DN or Kv2.2DN reduces  $I_K$  density in type I SCG cells by ~50%, whereas only Kv2.1DN expression attenuates  $I_K$  in type II cells. In addition, coexpression of Kv2.1DN and Kv2.2DN eliminates  $I_K$  in all type I cells and reduces  $I_K$  density in type II cells. Together with the biochemical data presented (Fig. 5), these results suggest that there are two distinct populations of Kv2.x-encoded  $I_K$  channels, and that these channels are differentially expressed: Kv2.1-encoded  $I_K$  channels in both type I and type II cells and Kv2.2-encoded  $I_K$  channels in

**Table 4. Effects of Kv2.1DN and Kv2.2DN expression on SCG neuron firing properties<sup>a</sup>**

Phenotype	$R_{in}(G\Omega)$	$V_m$ (mV)	$AP_{Thresh}$ (pA)	APA (mV)	APD <sub>50</sub> (msec)	APD <sub>90</sub> (msec)	<i>n</i>
<b>Wild type</b>							
All cells	0.34 ± 0.03	-48 ± 1	46 ± 5	82 ± 4	3.66 ± 0.14	5.92 ± 0.20	28
Phasic	0.26 ± 0.02	-45 ± 2	67 ± 1	80 ± 5	4.18 ± 0.24	6.55 ± 0.34	12
Adapting	0.60 ± 0.06	-48 ± 1	24 ± 2	87 ± 3	3.57 ± 0.20	5.96 ± 0.20	9
Tonic	0.22 ± 0.02	-52 ± 1	42 ± 2	91 ± 3	2.97 ± 0.03	4.87 ± 0.20	7
<b>Kv2.1DN</b>							
All cells	0.39 ± 0.04	-51 ± 1	36 ± 4	86 ± 3	3.60 ± 0.23	6.01 ± 0.38	24
Phasic	0.37 ± 0.02	-49 ± 1	49 ± 5	80 ± 2	3.78 ± 0.28	6.09 ± 0.37	10
Adapting	0.59 ± 0.06	-51 ± 2	31 ± 6	89 ± 5	3.63 ± 0.23	6.42 ± 0.34	8
Tonic	0.29 ± 0.04	-54 ± 1	36 ± 2	97 ± 2	3.21 ± 0.13	5.71 ± 0.18*	6
<b>Kv2.2DN</b>							
All cells	0.45 ± 0.10	-40 ± 2**	29 ± 3**	80 ± 3	3.48 ± 0.16	5.83 ± 0.36	29
Phasic	0.36 ± 0.03	-40 ± 4	45 ± 8**	67 ± 5	4.01 ± 0.29	6.36 ± 0.39	7
Adapting	0.74 ± 0.10	-35 ± 2**	26 ± 5	82 ± 2	3.42 ± 0.24	5.83 ± 0.35	14
Tonic	0.38 ± 0.08	-47 ± 1**	32 ± 3**	94 ± 1	3.11 ± 0.09	5.61 ± 0.19*	8
<b>Kv2.1DN plus Kv2.2DN</b>							
All cells	0.58 ± 0.06**	-41 ± 1**	25 ± 3**	76 ± 3	4.43 ± 0.25*	7.56 ± 0.43**	25
Phasic	0.40 ± 0.16	-42 ± 2	25 ± 3**	70 ± 4	4.90 ± 0.24	8.24 ± 0.39**	12
Adapting	0.63 ± 0.11	-36 ± 2**	25 ± 2	79 ± 6	4.02 ± 0.26	7.19 ± 0.41*	11
Tonic	0.33	-53	33	94	3.36	5.68	2

<sup>a</sup>All values are means ± SEM; \*\*\*Mean values are significantly different from those in wild-type cells at the \* $p < 0.02$  and \*\* $p < 0.005$  levels.

type I cells. To determine the effects of removing both populations of Kv2  $\alpha$ -subunit-encoded  $I_K$  channels, action potentials and repetitive firing patterns were recorded from SCG neurons expressing both Kv2.1DN and Kv2.2DN. Recordings from representative cells are shown in Figure 9. Several of the effects of Kv2.1DN and Kv2.2DN coexpression appear to be the sum of the effects of Kv2.1DN or Kv2.2DN expression alone. As in Kv2.2DN-expressing cells, for example, the mean ± SEM current threshold for action potential generation is decreased in cells expressing both dominant negative constructs. In addition, resting membrane potentials are depolarized in these cells compared with wild-type cells (Table 4). Interestingly, action potential durations in adapting ( $p < 0.02$ ) and phasic ( $p < 0.004$ ) Kv2.1DN plus Kv2.2DN-expressing cells are prolonged significantly, whereas expression of either Kv2.1DN or Kv2.2DN alone does not affect phasic and adapting action potential durations (Table 4). The most prominent effect of coexpression of both Kv2 dominant negative constructs, however, is the reduction of tonic cell number from 25% of wild-type SCG neurons to 8% of Kv2.1DN plus Kv2.2DN-expressing neurons. These observations are consistent with a role for  $I_K$  in action potential repolarization and in the regulation of tonic firing.

#### Expression of wild-type Kv2.1 $\alpha$ -subunits increases tonic firing

The results of the experiments described here suggest that Kv2-encoded  $I_K$  channels play a role in determining tonic firing. To explore this hypothesis further, action potentials and repetitive firing patterns were recorded from SCG cells transfected with wild-type Kv2.1 and EGFP (Fig. 10). These experiments revealed that the membrane properties of Kv2.1-transfected and wild-type phasic, adapting, and tonic SCG cells are indistinguishable (see on-line Table, available at [www.jneurosci.org](http://www.jneurosci.org)). However, expression of Kv2.1 markedly reduces the number of phasic (~25%) and adapting (~25%) cells and increases the number of tonic cells

(50%). In addition, mean ± SEM action potential durations at 50 and 90% repolarization in Kv2.1-expressing tonic cells are significantly ( $p < 0.02$ ) briefer than in phasic and adapting cells.

## DISCUSSION

### Two distinct components of $I_K$ encoded by Kv2.1 and Kv2.2 in SCG neurons

The studies described here were designed to probe the role of Kv2  $\alpha$ -subunits in the generation of voltage-gated  $K^+$  currents in SCG neurons. Biochemical experiments revealed that both Kv2.1 and Kv2.2 are expressed in SCG neurons, and that these  $\alpha$ -subunits do not appear to associate in these cells or in HEK-293 cells (Fig. 5). To explore the functional roles of Kv2  $\alpha$ -subunits, pore mutants of Kv2.1 (Kv2.1DN) and Kv 2.2 (Kv2.2DN), designed to function as dominant negatives, were constructed. Heterologous coexpression studies in HEK-293 cells revealed that the dominant negative effects of Kv2.1DN and Kv2.2DN are specific for Kv2.1 and Kv2.2 channels, respectively (Figs. 2, 3, Table 1). The simplest interpretation of these observations is that Kv2.1 and Kv2.2  $\alpha$ -subunits do not coassemble, at least in HEK-293 cells (Table 1). When expressed in SCG cells, Kv2.1DN selectively attenuates  $I_K$  in type I (expressing  $I_{AF}, I_K, I_{SS}$ ) and type II (expressing  $I_{AF}, I_{AS}, I_K, I_{SS}$ ) cells;  $I_{AF}, I_{AS}$ , and  $I_{SS}$  are unaffected by Kv2.1DN expression (Table 2). Expression of Kv2.2DN, in contrast, reduces  $I_K$  only in type I cells (Table 2).

The experiments here also revealed that the effects of Kv2.1DN and Kv2.2DN are additive. Coexpression of Kv2.1DN and Kv2.2DN, for example, eliminates  $I_K$  in type I SCG cells (Fig. 4, Table 2). Importantly, in these experiments, the total amount of cDNA used in the transfections was the same as with Kv2.1DN or Kv2.2DN alone. The additivity of the effects of Kv2.1DN and Kv2.2DN, therefore, does not simply reflect a dose-dependent attenuation of the current. Rather, the experimental observations suggest that Kv2.1DN and Kv2.2DN affect different populations of

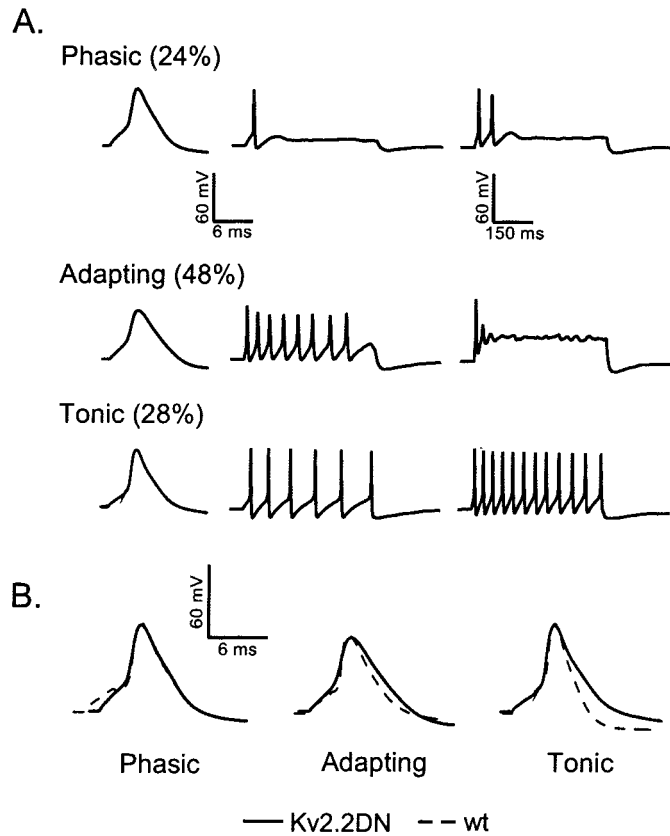


**Figure 8.** Expression of Kv2.2DN in SCG neurons increases the number of adapting cells. In SCG neurons transfected with Kv2.2DN (and EGFP), action potentials and repetitive firing patterns were recorded, and cells were classified as phasic (*top*), adapting (*middle*), or tonic (*bottom*), as described in the legend to Figure 7. Similar to the results obtained with Kv2.1DN, expression of Kv2.2DN prolongs action potential durations in tonic cells (*B*). In addition, Kv2.2DN expression alters the distribution of firing patterns: the percentage of phasic cells is reduced (by ~40%), and the percentage of adapting cells is increased (Table 4). *wt*, Wild type.

$I_K$  channels, consistent with the hypothesis that Kv2.1 and Kv2.2 do not coassemble in type I SCG neurons. The results presented here also reveal that Kv2-encoded  $K^+$  channels underlie  $I_K$  in all type I SCG neurons. In type II cells, in contrast,  $I_K$  is not eliminated with Kv2.1DN and Kv2.2DN coexpression. This might reflect the slow turnover rate of some Kv2.x-encoded  $K^+$  channels in type II SCG neurons. Alternatively, it is also possible that the expression levels of the dominant negative constructs were too low in these experiments to effectively eliminate  $I_K$  in type II cells. Both of these hypotheses seem unlikely, however, in light of the results obtained in type I cells and the similarities in the reductions in  $I_K$  in Kv2.1DN- and Kv2.1DN plus Kv2.2DN-expressing type II cells. It seems more likely that only a subset of  $I_K$  channels in type II cells are encoded by Kv2 (Kv2.1)  $\alpha$ -subunits, and that the residual  $I_K$  channels reflect the contribution of another  $Kv\alpha$ -subunit subfamily. Nevertheless, additional experiments aimed at determining the molecular identity of the individual  $I_K$  channels in type II cells will be necessary to test this hypothesis directly.

Kv2.1- and Kv2.2-encoded  $I_K$  channels are differentially expressed in type I and type II SCG cells: Kv2.1-encoded  $I_K$  is expressed in both type I and type II cells, whereas Kv2.2-encoded  $I_K$  channels are only evident in type I cells (Table 2). Although the numbers and the percentages of type III cells are small, the

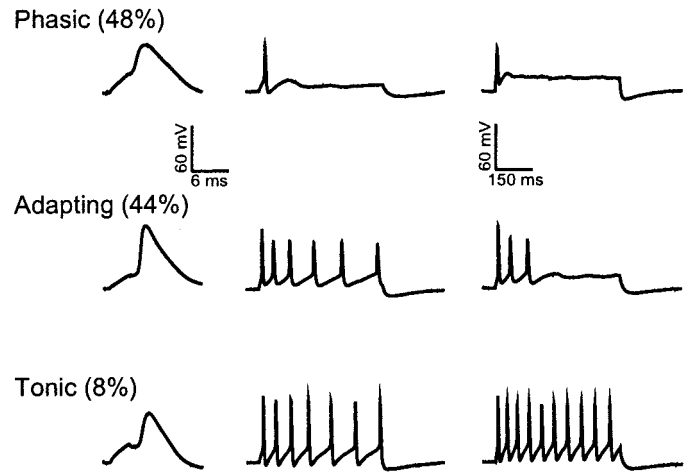


**Figure 9.** Coexpression of Kv2.1DN and Kv2.2DN markedly reduces tonic firing. Isolated SCG neurons were transfected with Kv2.1DN, Kv2.2DN, and EGFP. Action potentials and repetitive firing patterns were recorded, and cells were classified as phasic (*top*), adapting (*middle*), or tonic (*bottom*), as described in the legend to Figure 7. In contrast to the results obtained with expression of Kv2.1DN or Kv2.1DN alone (Figs. 7, 8), expression of both dominant negative constructs markedly decreases the percentage of tonic firing cells (Table 4).

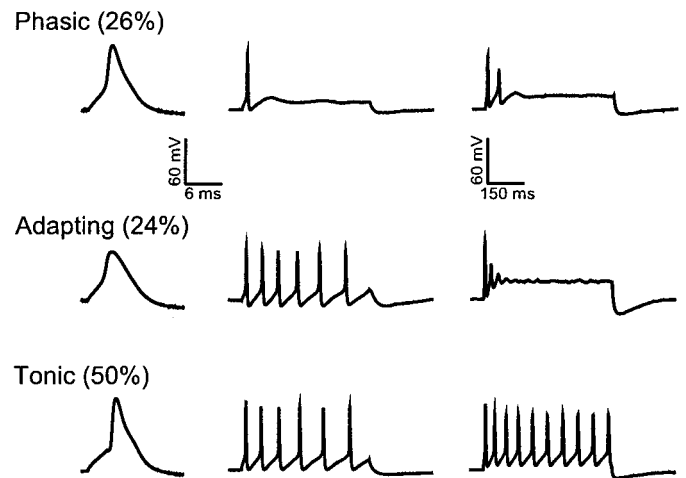


**Figure 10.** Expression of Kv2.1 in SCG neurons increases tonic firing. Action potentials and repetitive firing patterns, recorded as described in the legend to Figure 7, were obtained from isolated SCG neurons 24 hr after transfection with wild-type Kv2.1 and EGFP. As in wild-type cells, the phasic (*top*), adapting (*middle*), and tonic (*bottom*) firing patterns were seen in recordings from cells transfected with Kv2.1. However, the percentage of tonic cells is higher and the percentages of adapting and phasic cells are lower in Kv2.1-expressing cells than in either wild-type, Kv2.1DN-expressing (Fig. 7), or Kv2.2DN-expressing (Fig. 8) SCG cells (Table 4).

experiments completed to date suggest that  $I_K$  density is reduced in type III cells expressing Kv2.2DN but not in cells expressing Kv2.1DN (Table 2). No type III cells were seen in recordings from cells coexpressing Kv2.1DN and Kv2.2DN, an observation that likely reflects the small number ( $n = 16$ ) of cells studied in these experiments.

#### $I_K$ density regulates action potential repolarization and tonic firing

Expression of either Kv2.1DN or Kv2.2DN selectively increases action potential durations in tonic cells, suggesting that  $I_K$  chan-

nels contribute to action potential repolarization in these cells (Table 4). Although expression studies in *Xenopus* oocytes suggest relatively depolarized ( $\sim 0$  mV) thresholds for activation (Fink et al., 1996), Kv2.x-encoded  $K^+$  channels in mammalian cell lines activate at more depolarized (approximately  $-30$  to  $-40$  mV) potentials (Figs. 1, 2) (Murakoshi et al., 1997). In addition, action potential clamp experiments reveal substantial activation ( $\sim 20\%$  maximal) of Kv2.x-encoded currents in HEK-293 cells during a single (SCG) action potential (Fig. 6). Furthermore, expression of Kv2.1DN or Kv2.2DN markedly reduces the currents elicited during action potentials in SCG cells (Fig. 6). These results suggest an important role for Kv2.x-encoded  $K^+$  channels in action potential repolarization in SCG neurons and suggest that these channels, like other  $K^+$  channels, are differentially modified by expression environment (Peterson and Nerbonne, 1999). Interestingly, a similar conclusion was reached independently by Du et al. (2002) in studies focused on the functioning of Kv2.1-encoded currents in hippocampal neurons.

Although  $I_K$  shapes individual action potential waveforms in tonic cells, reductions in  $I_K$  density do not affect the percentage of cells that fire tonically (Table 4), revealing that brief action potentials are not the sole determinant of tonic firing. However, coexpression of Kv2.1DN and Kv2.2DN and the resulting reductions (in type II cells) or elimination (in type I cells) of  $I_K$  markedly reduce the percentage of tonic firing cells (Fig. 9). Although action potential repolarization in phasic and adapting cells is not affected by removal of either Kv2.1- or Kv2.2-encoded  $I_K$ , elimination of both Kv2.1- and Kv2.2-encoded  $I_K$  significantly ( $p < 0.001$ ) increases action potential durations in these cells (Table 4). Together, therefore, these observations suggest that  $I_K$  channels contribute to action potential repolarization in phasic, adapting, and tonic SCG cells, and that total  $I_K$  density is a critical determinant of the tonic firing pattern. Consistent with this hypothesis, expression of Kv2.1 increases  $I_K$  density and the percentage of tonic cells (see Fig. 10 and on-line Table, available at [www.jneurosci.org](http://www.jneurosci.org)).

### Kv2.2-encoded $I_K$ regulates neuronal excitability

Although both Kv2.1- and Kv2.2-encoded  $I_K$  channels play roles in action potential repolarization in SCG neurons, only Kv2.2-encoded  $I_K$  channels appear to contribute to the regulation of (resting) membrane excitability and to affect action potential firing. Expression of Kv2.2DN, for example, depolarizes all SCG cells and reduces the current thresholds for action potential generation in phasic and tonic cells (Table 4). Thus, unlike Kv2.1-encoded channels, Kv2.2-encoded  $I_K$  channels contribute to setting the resting membrane potentials of SCG neurons and function to regulate membrane excitability. Interestingly, the properties of Kv2.1- and Kv2.2-encoded  $K^+$  channels are very similar in heterologous expression systems (Figs. 1, 2), suggesting that there are cell-type-specific regulatory pathways that differentially modulate Kv2.1- and Kv2.2-encoded  $K^+$  channels. The functional distinctions between the Kv2.1- and Kv2.2-encoded  $I_K$  channels revealed in the experiments reported here suggest that differential regulation of these two  $I_K$  components, either by post-translational modification (Summers and Gelband, 1998; Colbert and Pan, 1999; Gelband et al., 1999; Zhu et al., 1999) or by coassembly with regulatory subunits (Chiara et al., 1999; Kerscheneister and Stocker, 1999), would have dramatically different effects on SCG cell membrane excitability. In addition, because Kv2.1- and Kv2.2-encoded  $I_K$  channels are differentially expressed in type I, type II, and type III SCG cells, differential

modulation of Kv2.x-encoded  $I_K$  channels would be expected to regulate neuronal excitability in a cell-type-specific manner. Additional experiments aimed at testing this hypothesis directly will clearly be of interest.

Previous studies have shown that the current thresholds for action potential generation are lower in adapting than in phasic or tonic cells, which appears to reflect, at least in part, the reduced density of the fast transient current  $I_{Af}$  in adapting cells (Malin and Nerbonne, 2000, 2001). The observations presented here that expression of Kv2.2DN reduces action potential thresholds and increases adapting cell number (Table 4) suggest a similar role of Kv2.2-encoded  $I_K$  channels. Furthermore, these results suggest that the adapting phenotype is correlated with low current thresholds for action potential generation, and that these low threshold values in adapting cells arise from reduced density of Kv2.2-encoded  $I_K$  (present study), as well as  $I_{Af}$  (Malin and Nerbonne, 2000, 2001), in these neurons.

### REFERENCES

- An WF, Bowlby MR, Betty M, Cao J, Ling H-P, Mendoza G, Hinson JW, Mattson KI, Strassle BW, Trimmer JS, Rhodes KJ (2000) Modulation of A-type potassium channels by a family of calcium sensors. *Nature* 403:553–556.
- Baranauskas G, Tkatch T, Surmeier JD (1999) Delayed rectifier currents in rat globus pallidus neurons are attributable to Kv2.1 and Kv3.1/3.2  $K^+$  channels. *J Neurosci* 19:6394–6404.
- Barry DM, Trimmer JS, Merlie JP, Nerbonne JM (1995) Differential expression of voltage-gated  $K^+$  channel subunits in adult rat heart. Relation to functional  $K^+$  channels. *Circ Res* 77:361–369.
- Barry DM, Xu H, Schuessler RB, Nerbonne JM (1998) Functional knock-out of the transient outward current, long-QT syndrome, and cardiac remodeling in mice expressing a dominant-negative Kv4  $\alpha$ -subunit. *Circ Res* 83:560–567.
- Blaine JT, Ribera AB (1998) Heteromultimeric potassium channels formed by members of the Kv2 subfamily. *J Neurosci* 18:9585–9593.
- Blaine JT, Ribera AB (2001) Kv2 channels form delayed-rectifier potassium channels *in situ*. *J Neurosci* 21:1473–1480.
- Chang JY, Martin DP, Johnson Jr EM (1990) Interferon suppresses sympathetic neuronal cell death caused by nerve growth factor deprivation. *J Neurochem* 55:436–445.
- Chiara MD, Monje F, Castellano A, Lopez-Barneo J (1999) A small domain in the N-terminus of the regulatory  $\alpha$ -subunit Kv2.3 modulates Kv2.1 potassium channel gating. *J Neurosci* 19:6865–6873.
- Coetzee WA, Amarillo Y, Chiu J, Chow A, Lau D, McCormack T, Moreno H, Nadal MS, Ozaita A, Pountney D, Saganich M, Vega-Saenz de Meira E, Rudy B (1999) Molecular diversity of  $K^+$  channels. *Ann NY Acad Sci* 868:233–285.
- Colbert CM, Pan E (1999) Arachadonic acid alters the availability of transient and sustained dendritic  $K^+$  channels in hippocampal CA1 pyramidal neurons. *J Neurosci* 19:8163–8171.
- Dixon JE, McKinnon D (1996) Potassium channel mRNA expression in prevertebral and paravertebral sympathetic neurons. *Eur J Neurosci* 8:183–191.
- Du J, Tao-Cheng J-H, Zerfas P, McBain CJ (1998) The  $K^+$  channel, Kv2.1, is apposed to astrocytic processes and is associated with inhibitory post-synaptic membranes in hippocampal and cortical principal neurons and inhibitory interneurons. *Neuroscience* 84:37–48.
- Du J, Haak LL, Phillips-Tansey E, Russell JT, McBain CJ (2000) Frequency-dependent regulation of rat hippocampal somato-dendritic excitability by the  $K^+$  channel subunit Kv2.1. *J Physiol (Lond)* 522:19–31.
- Fink M, Duprat F, Lesage F, Heurteaux C, Romey G, Barhanin J, Lazdunski ML (1996) A new  $K^+$  channel  $\beta$  subunit to specifically enhance Kv2.2 (CDRK) expression. *J Biol Chem* 271:26341–26348.
- Gelband CH, Warth JD, Mason HS, Zhu M, Moore JM, Kenyon JL, Horowitz B, Summers C (1999) Angiotensin II type 1 receptor-mediated inhibition of  $K^+$  channel subunit Kv2.2 in brain stem and hypothalamic neurons. *Circ Res* 84:352–359.
- Hwang PM, Glatt CE, Bredt DS, Yellen G, Snyder SH (1992) A novel  $K^+$  channel with unique localizations in mammalian brain: molecular cloning and characterization. *Neuron* 8:473–481.
- Hwang PM, Fotuhi M, Bredt DS, Cunningham AM, Snyder SH (1993) Contrasting immunohistochemical localizations in rat brain of two novel  $K^+$  channels of the *Shab* subfamily. *J Neurosci* 13:1569–1576.
- Kerscheneister D, Stocker M (1999) Heteromeric assembly of Kv2.1 with Kv9.3: effect on the state dependence of inactivation. *Biophys J* 77:248–257.

- Kuryshv YA, Gudz TI, Brown AM, Wible BA (2000) KChAP as a chaperone for specific  $K^+$  channels. *Am J Physiol* 278:C931–C941.
- Li H, Guo W, Nerbonne JM (1999) Functional consequences of cardiac-specific expression of wild-type or mutant (dominant negative) Kv1.5  $\alpha$ -subunits in mouse ventricular myocytes. *Circulation* 102:2–261.
- Lim ST, Antonucci DE, Scannevin RH, Trimmer JS (2000) A novel targeting signal for proximal clustering of the Kv2.1  $K^+$  channel in hippocampal neurons. *Neuron* 25:385–397.
- Maletic-Savatic M, Lenn NJ, Trimmer JS (1995) Differential spatiotemporal expression of  $K^+$  channel polypeptides in rat hippocampal neurons developing *in situ* and *in vitro*. *J Neurosci* 15:3840–3851.
- Malin SA, Nerbonne JM (2000) Elimination of the fast transient in superior cervical ganglion neurons with expression of Kv4.2W362F: molecular dissection of  $I_A$ . *J Neurosci* 20:5191–5199.
- Malin SA, Nerbonne JM (2001) Molecular heterogeneity of the voltage-gated fast transient outward  $K^+$  current,  $I_{AF}$ , in mammalian neurons. *J Neurosci* 21:8004–8014.
- Murakoshi H, Trimmer JS (1999) Identification of the Kv2.1  $K^+$  channel as a major component of the delayed rectifier  $K^+$  current in rat hippocampal neurons. *J Neurosci* 19:1728–1735.
- Murakoshi H, Shi G, Scannevin RH, Trimmer JS (1997) Phosphorylation of the Kv2.1  $K^+$  channel alters voltage dependent activation. *Mol Pharmacol* 52:821–828.
- Pankevyh H, Kristufek D, Huck S (1999) Perinatal and postnatal regulation of Shaker-related genes in rat superior cervical ganglion. *Soc Neurosci Abstr* 25:739.1.
- Petersen KR, Nerbonne JM (1999) Expression environment determines  $K^+$  current properties: Kv1 and Kv4  $\alpha$  subunit-induced  $K^+$  currents in mammalian cell lines and cardiac myocytes. *Pflügers Arch* 437:381–392.
- Pond AL, Scheve BK, Benedict AT, Petrecca K, Van Wagoner DR, Shrier A, Nerbonne JM (2000) Expression of distinct ERG proteins in rat, mouse, and human heart: relation to functional  $I_{Kr}$  channels. *J Biol Chem* 275:5997–6006.
- Pongs O (1999) Voltage-gated potassium channels: from hyperexcitability to excitement. *FEBS Lett* 452:31–35.
- Raff MC, Fields KL, Hakomori S-I, Mirsky R, Pruss RM, Winter J (1979) Cell-type-specific markers for distinguishing and studying neurons and the major classes of glial cells in culture. *Brain Res* 174:283–308.
- Rudy B (1988) Diversity and ubiquity of K channels. *Neuroscience* 24:729–749.
- Storm JF (1990) Potassium currents in hippocampal pyramidal cells. *Prog Brain Res* 83:161–187.
- Summers C, Gelband CH (1998) Neuronal ion channel signaling pathways: modulation by angiotensin II. *Cell Signal* 10:303–311.
- Trimmer JS (1991) Immunological detection and characterization of a delayed rectifier  $K^+$  channel polypeptide in rat brain. *Proc Natl Acad Sci USA* 88:10764–10768.
- Zhu M, Gelband CH, Posner P, Summers C (1999) Angiotensin II decreases neuronal delayed rectifier potassium current: role of calcium/calmodulin-dependent protein kinase II. *J Neurophysiol* 82:1560–1568.